MORE REALISTIC CONSIDERATION OF BACKSHEETS COEFFICIENT OF THERMAL EXPANSION ON THERMOMECHANICS OF PV MODULES

Pascal Romer[1], Gernot Oreski[2], Andreas J. Beinert[1], Holger Neuhaus[1], Max Mittag[1]
[1]Fraunhofer Institute for Solar Energy Systems ISE, Heidenhofstraße 2, 79110 Freiburg, Germany;
[2]Polymer Competence Center Leoben GmbH, Roseggerstraße 12, A-8700 Leoben, Austria;
Corresponding author: Pascal Romer | Phone: +49 (0)761 4588 5044 | E-mail: Pascal.Romer@ise.fraunhofer.de

ABSTRACT: This paper deals with the effect of anisotropic and negative thermal expansion of polymeric backsheets. Even though these effects are well known in polymer engineering, so far they have not been considered in FEM simulation of PV modules. Therefore, we investigate the influence of those effects on the thermomechanical stress in PV modules after lamination and for mechanical load as well as thermal cycling. With the anisotropic partially negative coefficient of thermal expansion (CTE) the general shape of the third principal stress after lamination changes to a more asymmetric one. The probability of cell fracture after mechanical loading changes with the compressive stress after lamination. It ranges from 5 % for the AAA backsheet up to 55 % for the APA. This leads to the conclusion that the anisotropic, partially negative CTE of backsheets is not negligible and should be considered in all thermomechanical simulations of PV modules.

Keywords: Finite element modelling, FEM simulations, photovoltaic module, backsheet, stress, thermomechanics, mechanical load, virtual prototyping.

1 INTRODUCTION

Anisotropic behavior of polymer films is common for thermoplastic materials as the polymer chains tend to align in extrusion direction depending on the processing conditions (e.g. temperature and shear). When cooling down from the melt the aligned polymer chains have thermodynamic imbalances in the amorphous phase below the glass transition temperature. Polymer materials try to overcome this imbalance to reach balanced conditions. Exposure to higher temperature near the glass transition or melting region leads to relaxation of chain orientations causing either shrinkage or internal stress during lamination or operation. Over the long term, this effect can lead to delamination or even cracking of the backsheet as it was observed for cracking of polyamide backsheets [2].

The anisotropic and negative coefficient of thermal expansion (CTE) of polymer films is a well-known phenomenon in polymer engineering [2], but the influence on the thermomechanical stress in PV modules has not yet been investigated.

From our knowledge, all FEM models use an isotropic and temperature independent CTE for the backsheet. To obtain a more accurate model we consider the anisotropy as well as the temperature dependency of the backsheet. Therefore, we include the measured CTEs for different backsheets and thermal treatments of them into our FEM model and compare the simulation to the previously used material model.

2 METHOD

2.1 CTE measurement

The CTE is measured using a Danteq Q400 Digital Image Correlation (DIC) system. Digital Image Correlation (DIC) systems enable contactless and precise measurement of thermally and/or mechanically induced strains of thin as well as anisotropic layers [3, 4]. DIC systems are optical strain measurement systems, using a camera setup and specimens with a random speckle pattern. The camera(s) can track this specific speckle pattern and hence the deformations of samples during loading can be measured similarly in two directions.

The samples are placed horizontally on a hotplate. The hotplate is placed within a concealed temperature chamber. All DIC samples are painted with the necessary speckle pattern. First, the samples were coated with a white primer. Afterwards, the pattern was applied using a dedicated black graphite DIC aerosol lacquer. In order to obtain information on reversible and irreversible changes in the materials, two heating runs were carried out. The first heating run from room temperature to 150 °C measures the CTE of the backsheets as received from manufacturing. After cooling down to room temperature, in the second heating run the effect of module lamination temperature on the CTE of the backsheets is determined. All CTE measurements are done between 20 °C and 150 °C.

2.2 FEM simulation

The FEM model is based on previous studies with neglected metallization and ribbons [3]. Due to the twofold axis symmetry a quarter of a 60-cell PV module with full square solar cells is simulated. We simulate lamination, thermal cycling (TC) and mechanical load (ML). In each simulation step the four measured backsheets with an anisotropic, partially negative CTE are used (see Fig. 1) and compared to one reference simulation with an isotropic, non-negative CTE. The lamination process is simulated using a single temperature drop from 150 °C to 25 °C, with the CTE of the first heating run of the measurement. The residual stress state is used as an initial condition for the TC and ML simulation. A frame is considered in latter simulations. Similar to the lamination, the TC is simulated as a single temperature drop from 25 °C to -40 °C followed by a temperature jump up to 85 °C, where the CTE of the second heating measurement is used. ML is simulated at 25 °C with a homogeneous push load of 2400 Pa and 5400 Pa. The material parameters used in the simulation are shown in Table 1. To only investigate the influence of the different CTEs all other material parameters of the backsheet are kept constant throughout the simulations.

The analysis focuses on the principal stresses in the solar cells. Due to the brittleness of silicon, solar cells tend to break under tensile stress. To compare the effect of the backsheet's CTE we calculate the probability of solar cell fracture P_f using the Weibull distribution [4] considering size effects [5]:

$$P_\mathrm{f} = 1 - \exp\left(\sum_\mathrm{i} -A_\mathrm{eff,i}\left(\frac{\sigma_\mathrm{I,max}}{\sigma_\mathrm{0,i}}\right)^{m_\mathrm{i}}\right), \qquad (1)$$

where A_eff is the effective area, $\sigma_\mathrm{I,max}$ the maximum first principal stress, σ_0 the Weibull scale factor and m the Weibull modulus. The effective area A_eff can be interpreted as an equivalent area where the maximum first principal stress $\sigma_\mathrm{I,max}$ occurs. It is calculated via:

$$A_\mathrm{eff,i} = \int \left(\frac{\sigma_\mathrm{I,i}(\mathrm{x},\mathrm{y})}{\sigma_\mathrm{I,max}}\right)^{m_\mathrm{i}} dA_\mathrm{i}\,, \qquad (2)$$

where the first principal stress $\sigma_\mathrm{I,i}(\mathrm{x},\mathrm{y})$ at the position (x,y) is integrated over the surface $A_\mathrm{i}(\mathrm{x},\mathrm{y})$. The probability of solar cell fracture P_f is the expected value of the existence of at least one crack in at least one cell of the PV module. The Weibull scale factor σ_0 and modulus m are taken from Kaule, *et al.* for a certain cell production process [6].

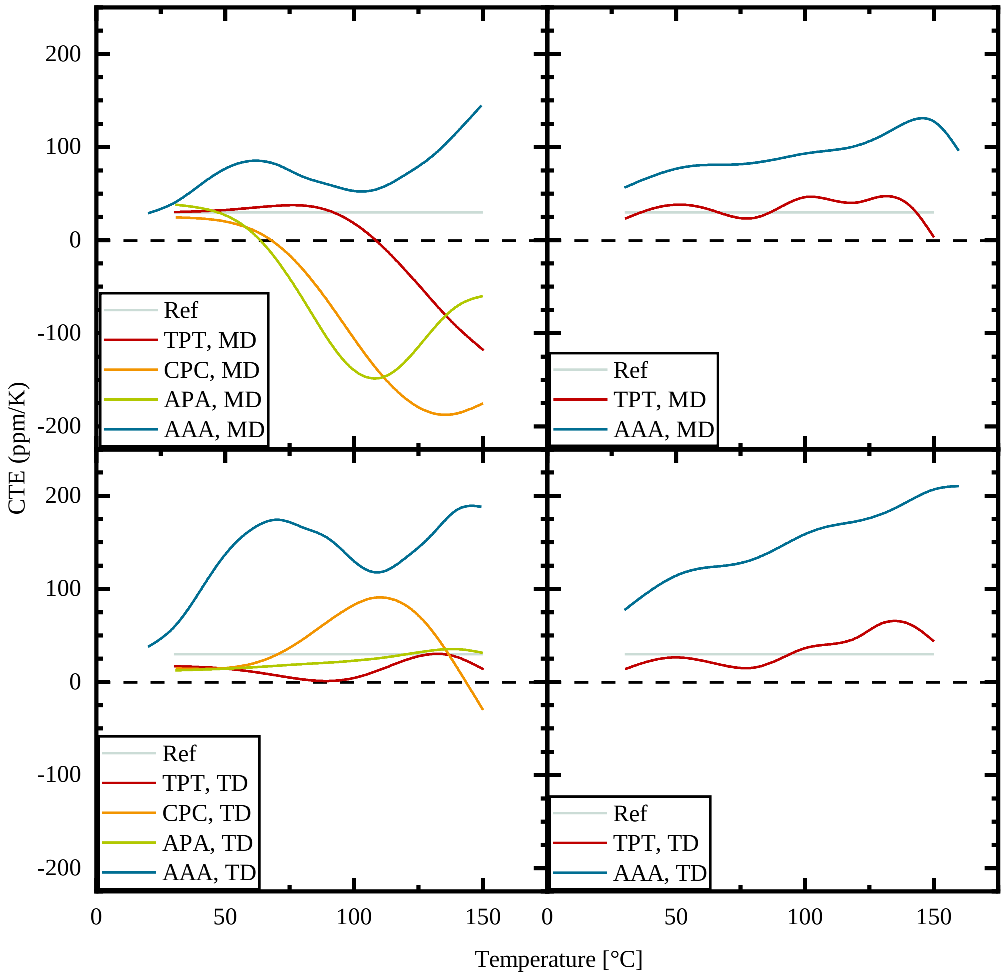

Fig. 1: CTE measurement of the first (left) and second heating (right) in machine direction (top) and transversal direction (bottom) for the four different backsheets. For the CPC and APA backsheets only the first heating was possible due to deformation of the backsheets.

Table 1: Specifications and material properties of the PV module. *: provided by manufacturer, †: measured.

Layer	Material	Dimension	Density [g/cm³]	Young's modulus [GPa]	Poisson's ratio [-]	CTE [10^{-6}K^{-1}]
Front glass	soda-lime glass	3.2 mm	2.5*	70*	0.2*	9*
Encapsulant	EVA	460 µm	0.96 [1]	T-dep.†	0.4 [1]	270 [1]
Solar cell	Cz-silicon	156.75 × 156.75 × 0.180 mm³	2.329 [1]	Elasticity matrix [1]		T-dep. [7, 8]
Backsheet	APA,TPT, CPC, AAA	295 µm	2.52 [1]	3.5 [1]	0.29 [1]	T-dep.†
Frame	aluminium		2.7 [9]	70 [9]	0.33 [9]	23 [9]
Frame-inlay	rubber	8.85 × 1.15 mm²	0.067*	0.0074*	0.3*	769*

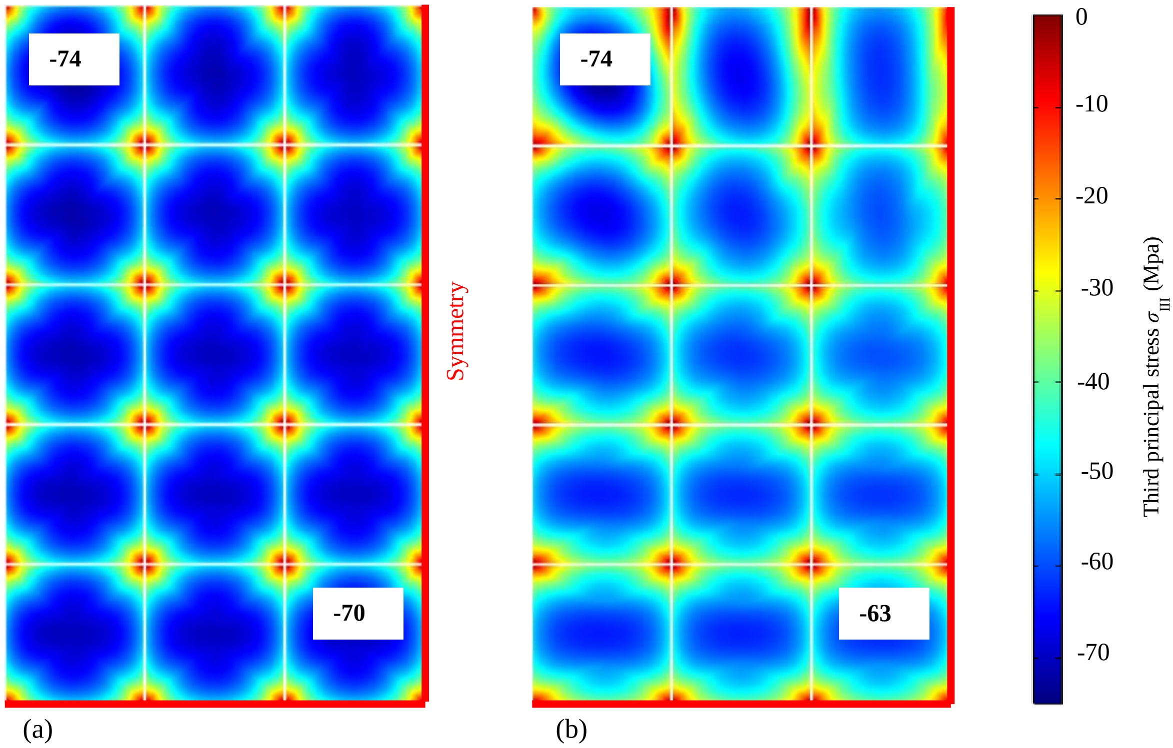

Fig. 2: Third principal stress after lamination for the isotropic (a) and the anisotropic (b) material model of the CPC backsheet. The symmetry axes of the PV-module are marked by red lines. For the inner cells the third principal stress after lamination is about 7 MPa lower for the anisotropic material model compared to the isotropic one.

3 RESULTS

3.1 CTE measurements

In the first heating run, all investigated backsheets (tedlar-PET-tedlar (TPT), coated PET (CPC), polyamide-PET-polyamide (APA), polyamide-polyamide-polyamide (AAA)) show anisotropic or even negative thermal expansion (Fig. 1). The extend of the effect is dependent on the polymers used, especially on the thermal transitions of the materials.

For the PET containing backsheets, shrinkage in machine direction (MD) and expansion perpendicular to it (TD) is observed. This anisotropy can be attributed to the biaxial stretching during film production, which is done in order to increase thermo-mechanical stability and hydrolysis resistance. Moreover, an influence of the glass transition (between 70 °C and 100 °C) and the degree of biaxial stretching is observable, resulting in partially negative CTE values in the glass transition region.

The co-extruded polyamide backsheet shows less anisotropy, with expansion in both directions. Other than the PET based backsheets, which have CTE values smaller than 50 ppm K^{-1}, the AAA backsheet exhibits values up to 200 ppm K^{-1} to a temperature of 60 °C.

The second heating run simulates the effect of PV module lamination on the thermal expansion behavior of the backsheets. In comparison to the first heating run, TPT did not show shrinkage or negative CTE values anymore, indicating that during PV module lamination the chain orientations exhibit relaxation. Moreover, the degree of anisotropy is significantly reduced.

The AAA backsheet also showed relaxation effects. Whereas in the first heating run between 50 and 100 °C shrinkage due to relaxation of orientations (but no negative CTE values) was observed, in the 2nd heating a more or less constant expansion was measured until 150 °C.

Unfortunately no CTE values for the APA backsheet could be measured, as the film sample showed significant warpage. Nevertheless, warpage is a qualitative indicator for the internal stresses that have been released during heating above the glass transition of the PET core layer.

3.2 Lamination

Fig. 2 shows the third principal stress after lamination for the isotropic (a) and the anisotropic, partially negative (b) CTE of the APA backsheet. In the isotropic case a symmetric distribution of the third principal stress σ_{III} at every cell is observed. Whereas the anisotropic material model leads to an asymmetric stress distribution. Table 2 shows the maximum third principal stress at the innermost cell after lamination for the different backsheets. The AAA backsheet has the highest compressive stress (-103 MPa) due to the strictly positive CTE. The other backsheets (TPT, CPC, APA), with their partly negative CTE show a much lower third principal stress. The reference simulation, with an constant, isotropic CTE, shows a comparable stress level to the TPT backsheet.

Table 2: Maximal third principal stress after lamination at the innermost cell for the different backsheets

Backsheet	Reference	TPT	CPC	APA	AAA
σ_{III} [MPa]	-70	-73	-63	-63	-103

3.3 Mechanical load

The maximum first principal stress for a mechanical push load of 2400 Pa and 5400 Pa for the reference (grey) and the anisotropic material models strongly depends on the used CTE (Fig. 3). The difference in the tensile stress after mechanical load are caused by the difference of the compressive stress after lamination. Therefore the AAA backsheet with the highest compressive stress shows the lowest tensile stress. At 2400 Pa the different CTEs result in an increase from 6 MPa for the AAA backsheet and up to 44 MPa for the APA backsheet. At 5400 Pa the tensile stress rises even more significant, with 47 MPa, from 110 MPa up to 157 MPa. The probability of cell fracture at 2400 Pa is negligible for all used CTEs In contrast, the probability of cell fracture is relevant at a push load of 5400 Pa. It ranges from 5 % for the AAA backsheet up to 55 % for the APA backsheet. Therefore, the CTE has an indirect but significant influence on the tensile stress during mechanical load and thus has to be considered carefully.

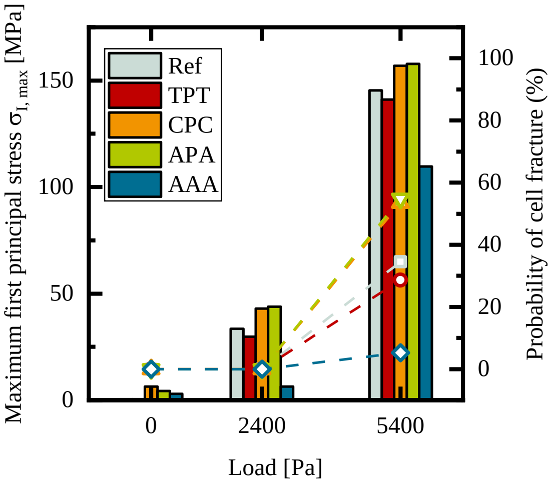

Fig. 3: Resulting maximum first principal stress (bars, left axis) and probability of cell fracture (dashed line, right axis) for the different backsheets at 0, 2400 and 5400 Pa mechanical push load.

3.4 Thermal cycles

Mainly compressive stress occurs during thermal cycling due to the neglected interconnector. Fig. 4 shows the results for the reference simulation as well as the TPT and the AAA backsheet. Due to the glass transition of the encapsulant at approximately -20 °C the compressive stress increases significantly below this temperature. The whole thermal cycling process takes place below the glass transition temperature of the PET core of the backsheets, therefore the TPT simulation is comparable to the reference. In comparison to that, the AAA with its much higher CTE shows higher compressive stress values during thermal cycling. Furthermore the initial stresses in the backsheets are relaxed due to the first heating of the lamination process. Therefore no more anisotropic stress distribution is observable.

4 CONCLUSIONS

All investigated backsheets show anisotropic thermal expansion. For the PET containing backsheets, shrinkage in machine direction (MD) and expansion perpendicular to it (TD) is observed. Moreover, an influence of the glass transition (between 70 °C and 100 °C) and the degree of biaxial stretching is observable, resulting in partially negative CTE values in the glass transition region. The co-extruded polyamide (PA) backsheet shows much less anisotropy, with expansion in both directions.

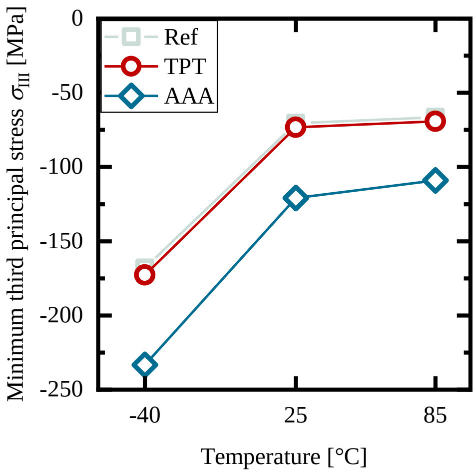

Fig. 4: Minimum third principal stress during thermal cycling for the TPT and AAA backsheet

The FEM simulation of the lamination process shows a large effect of the backsheets' CTE on the resulting third principal stress. It ranges from -63 MPa (CPC and APA) up to -103 MPa (AAA). It is shown with simulation that the different stress states after lamination will influence the mechanical load test. The AAA backsheet has the lowest probability of cell fracture of 5 %. It increases to over 20 % (TPT) and up to 55 % for the APA and CPC backsheets, respectively. We conclude that the CTE with its anisotropy and partly negative areas should be considered exactly in further FEM simulations.

5 REFERENCES

[1] U. Eitner, S. Kajari-Schroeder, M. Koentges, and H. Altenbach, "Thermal stress and strain of solar cells in photovoltaic modules," in *Advanced Structured Materials*, vol. 15, *Shell-like Structures: Non-classical Theories and Applications*, H. Altenbach and V. A. Eremeyev, Eds., Berlin/Heidelberg: Springer, 2011.

[2] G. C. Eder *et al.*, "Error analysis of aged modules with cracked polyamide backsheets," *Solar Energy Materials and Solar Cells*, vol. 203, p. 110194, 2019, doi: 10.1016/j.solmat.2019.110194.

[3] A. J. Beinert, P. Romer, M. Heinrich, M. Mittag, J. Aktaa, and H. Neuhaus, "The Effect of Cell and Module Dimensions on Thermomechanical Stress in PV Modules," *IEEE J. Photovoltaics*, vol. 10, no. 1, pp. 70–77, 2020, doi: 10.1109/JPHOTOV.2019.2949875.

[4] W. Weibull, *A Statistical Theory of the Strength of Materials*. Stockholm: Generalstabens Litografiska Anstalts Förlag, 1939.

[5] D. Munz and T. Fett, *Ceramics: Mechanical properties, failure behaviour, materials selection*, 1st ed. Berlin | Heidelberg: Springer, 2001.

[6] F. Kaule, M. Pander, M. Turek, M. Grimm, E. Hofmueller, and S. Schoenfelder, "Mechanical damage of half-cell cutting technologies in solar cells and module laminates," in *SiliconPV 2018,*

The 8th International Conference on Crystalline Silicon Photovoltaics: Conference date, 19-21 March 2018 : location, Lausanne, Switzerland, 2018, p. 20013.
[7] R. B. Roberts, “Thermal expansion reference data: silicon 300-850 K,” *Journal of Physics D: Applied Physics*, vol. 14, no. 10, L163-163, 1981.
[8] R. B. Roberts, “Thermal expansion reference data: silicon 80-280K,” *Journal of Physics D: Applied Physics*, vol. 15, no. 9, L119-120, 1982.
[9] W. M. Haynes, Ed., *CRC handbook of chemistry and physics*: CRC Press, 2014.